



Published in final edited form as:

Am J Surg Pathol. 2018 November ; 42(11): 1562–1570. doi:10.1097/PAS.0000000000001140.

Novel *MEIS1-NCOA2* Gene Fusions Define a Distinct Primitive Spindle Cell Sarcoma of the Kidney

Pedram Argani, MD¹, Victor E. Reuter, MD², Payal Kapur, MD³, James E. Brown, MD⁴, Yun-Shao Sung, MS², Lei Zhang, MD², Richard Williamson, MD⁵, Glen Francis, MD⁵, Scott Sommerville, MD⁶, David Swanson, BSc⁷, Brendan C. Dickson, MD⁷, Cristina R. Antonescu, MD²

¹Departments of Pathology and Oncology, Johns Hopkins University School of Medicine, Baltimore, Maryland, USA

²Department of Pathology, Memorial Sloan Kettering Cancer Center, New York, NY, USA

³Department of Pathology, University of Texas Southwestern Medical Center, Dallas, TX, USA

⁴Department of Pathology, West Jefferson Medical Center, Marrero, LA, USA

⁵Medlab Pathology, Brisbane, Australia

⁶Orthopedic Surgery, The Joint Space, Auchenflower Qld, Australia

⁷Department of Pathology and Laboratory Medicine, Mount Sinai Hospital, Toronto, Ontario, Canada

Abstract

We describe two cases of a distinct sarcoma characterized by a novel *MEIS1-NCOA2* gene fusion. This gene fusion was identified in the renal neoplasms of two adults (21 year-old male, 72 year-old female). Histologically, the resected renal neoplasms had a distinctively nodular appearance, and while one renal neoplasm was predominantly cystic, the other demonstrated solid architecture, invasion of perirenal fat, and renal sinus vasculature invasion. The neoplasms were characterized predominantly by monomorphic plump spindle cells arranged in vague fascicles with a whorling pattern; however, a more primitive small round cell component was also noted. Both neoplasms were mitotically active and one case showed necrosis. The neoplasms did not have a distinctive immunohistochemical profile, though both labeled for TLE1. The morphologic features are distinct from other sarcomas associated with *NCOA2* gene fusions, including mesenchymal chondrosarcoma, congenital/infantile spindle cell rhabdomyosarcoma, and soft tissue angiofibroma. While we have minimal clinical follow-up, the aggressive histologic features of these neoplasms indicate malignant potential, thus warranting classification as a novel subtype of sarcoma.

Correspondence: Pedram Argani, M.D., The Johns Hopkins Hospital, Surgical Pathology, Weinberg Building, Room 2242, 401 N. Broadway, Baltimore, Maryland 21231-2410, pargani@jhmi.edu; Tel# (410) 614-2428, Fax# (410) 955-0115, Cristina R. Antonescu, MD, Memorial Sloan Kettering Cancer Center, 1275 York Ave, New York, NY 10021, antonesc@mskcc.org.

Keywords

Renal Neoplasm; sarcoma; *MEIS1*; *NCOA2*; Translocation

INTRODUCTION

Perhaps more than any other visceral organ, the kidney is the site of origin of many translocation-associated sarcomas, which follow closely the paradigm seen in soft tissue tumors. Many of these neoplasms present in children and young adults, though a smaller proportion does affect adults. Some examples of translocation associated sarcomas which present as primary renal neoplasms include cellular congenital mesoblastic nephroma/infantile fibrosarcoma¹⁻³, Ewing sarcoma/primitive neuroectodermal tumor (ES/PNET)⁴⁻⁵, synovial sarcoma⁶, sclerosing epithelioid fibrosarcoma⁷, desmoplastic small round tumor (DSRCT)⁸, clear cell sarcoma/melanoma of soft parts⁹, and Xp11 translocation perivascular epithelioid cell tumor (PEComa)/melanotic Xp11 translocation renal cancer¹⁰⁻¹¹. More recently, a subset of renal sarcomas which overlap with clear cell sarcoma of the kidney (CCSK) have been shown to harbor *BCOR-CCNB3*¹² or *YWHAE-NUTM2B*¹³ gene fusions rather than the *BCOR* internal tandem duplication¹⁴ harbored by most cases of CCSK. Despite these advances, many primary renal sarcomas remain unclassified.

In this report we describe two cases of primary renal sarcoma harboring a novel *MEIS1-NCOA2* gene fusion. Their distinctive shared morphologic features and distinct gene fusion support the idea that they represent a novel sarcoma entity.

METHODS

Cases

The two renal cases reported herein were retrieved from the consultation files of two authors (PA, VER). Cases were identified during a review of unclassified primary renal sarcomas, which was aimed at identifying those with *BCOR-CCNB3* gene fusion¹². A total of 22 such cases were studied. Case one was sent for RNA-sequencing which revealed a *MEIS1-NCOA2* gene fusion candidate. This result was validated with FISH using custom BAC probes, showing break-apart signals in both *MEIS1* and *NCOA2* genes. The remaining cases were then screened by FISH to identify potential *NCOA2* gene fusions. This resulted in the identification of case#2, which was shown by FISH to harbor *NCOA2* and *MEIS1* gene rearrangements.

Fluorescence in Situ Hybridization (FISH)

FISH on interphase nuclei from paraffin-embedded 4-micron sections was performed applying custom probes using bacterial artificial chromosomes (BAC), covering and flanking genes that were identified as potential fusion partners in the RNA-seq experiment. BAC clones were chosen according to UCSC genome browser (<http://genome.ucsc.edu>), see Supplementary Table 1. The BAC clones were obtained from BACPAC sources of Children's Hospital of Oakland Research Institute (CHORI) (Oakland, CA) (<http://bacpac.chori.org>) and Life Technologies Corporation (Carlsbad, CA). DNA from individual

BACs was isolated according to the manufacturer's instructions, labeled with different fluorochromes in a nick translation reaction, denatured, and hybridized to pretreated slides. Slides were then incubated, washed, and mounted with DAPI in an antifade solution, as previously described¹⁵. The genomic location of each BAC set was verified by hybridizing them to normal metaphase chromosomes. Two hundred successive nuclei were examined using a Zeiss fluorescence microscope (Zeiss Axioplan, Oberkochen, Germany), controlled by Isis 5 software (Metasystems, Newton, MA). A positive score was interpreted when at least 20% of the nuclei showed a break-apart signal. Nuclei with incomplete set of signals were omitted from the score.

RNA Sequencing

RNA was extracted from formalin-fixed paraffin-embedded (FFPE) tissue using Amsbio's ExpressArt FFPE Clear RNA Ready kit (Amsbio LLC, Cambridge, MA). Fragment length was assessed with an RNA 6000 chip on an Agilent Bioanalyzer (Agilent Technologies, Santa Clara, CA). RNA-sequencing libraries were prepared using 20 to 100 ng total RNA with the TruSight RNA Fusion Panel (Illumina, San Diego, CA). Each sample was subjected to targeted RNA sequencing on an Illumina MiSeq at 8 samples per flow cell (~3 million reads per sample). All reads were independently aligned with STAR (version 2.3) and BowTie2 against the human reference genome (hg19) for Manta-Fusion and TopHat-Fusion analysis, respectively.

For comparison of mRNA expression profiles, we included two mesenchymal chondrosarcomas with known *HEY1-NCOA2* gene rearrangements, and one soft tissue angiofibroma with a known *AHRR-NCOA2* gene fusion. In addition, unsupervised clustering was performed including the renal index case (Case 1), three other control cases with *NCOA2* gene fusions (2 mesenchymal chondrosarcomas, 1 soft tissue angiofibroma), and over 100 other sarcomas available on the same targeted RNA-sequencing platform¹⁶.

Other Neoplasms Tested for MEIS1-NCOA2 fusion by FISH

We studied additional tumor types which could potentially be related to the current cohort of *MEIS1-NCOA2* positive sarcomas. First, we investigated a group of 11 typical adult mixed epithelial stromal tumor/cystic nephroma (MEST/CN) and 2 pediatric CN, which were previously described in detail in a recent study from our group¹⁷. The adult MEST/CN occurred in females with an age range of 11 to 73 years, and had the typical morphologic features of MEST/CN, including cellular stroma, wavy collagen, and estrogen receptor immunoreactivity¹⁷. The two pediatric CN occurred in males 1 and 2 years of age. Second, we also studied 4 cases of mesenchymal chondrosarcoma and 1 angiofibroma with proven *NCOA2* gene rearrangements but unknown partner from the consultation files of one author (CRA).

RESULTS

Clinical History and Gross Appearance

Case 1 was a 72 year-old female with cystic left renal tumor that was removed by partial nephrectomy. The neoplasm proved to be a 4 cm complex cyst with an average wall

thickness of 1 mm, but with multiple clear to yellow-tan excrescences projecting within cyst lumens. Margin status was unclear as the specimen was received with a defect that connected to the cyst. At 9 months follow-up, there is no evidence of recurrent disease.

Case 2 was a 21 year-old male who was found to have a 15 cm left renal mass and underwent radical nephrectomy. One sectioning, the neoplasm was pale-tan to white, and was solid, nodular, and friable with multiple areas of necrosis and hemorrhage. The tumor involved an area of disruption at the capsular margin. The patient was lost to follow-up.

MEIS1-NCOA2 positive renal neoplasms show a primitive spindle cell phenotype with a distinctive whorling and nodular pattern and non-specific immunoprofile.

The most distinctive feature of the resected renal neoplasms was their nodular growth pattern. This was created by spindle cells arranged in short fascicles with a distinct whorling pattern (Figures 1, 2). The spindled cells were monomorphic, short, and plump with scant amounts of pink cytoplasm. A population of more primitive rounded cells was also present, typically centered on capillary vasculature.

While the most common phenotype of the neoplastic cells was that of a plump spindle cell, variant patterns were present in each case. Case 2 additionally had an epithelioid-round cell component, raising the differential of a primitive round cell sarcoma. Homer Wright pseudorosette-like structures were noted reminiscent of primitive neuroectodermal tumor (PNET) (Figure 2G). Case 1 had better formed fascicles composed of elongated spindled cells in a fibrous background, mimicking the appearance of monophasic synovial sarcoma (Figure 1C).

Both neoplasms entrapped native renal tubules at their periphery. In case 1, this was the dominant appearance, such that the lesion presented as multicystic mass. The neoplastic spindle cells surrounded cystically dilated entrapped native renal tubular epithelium; the latter frequently had a hobnail appearance characterized by prominent eosinophilic cytoplasm and apically oriented, enlarged nuclei with vesicular chromatin, suggesting the possibility of malignant transformation of mixed epithelial stromal tumor/cystic nephroma (MEST/CN) (Figure 1G). In other areas, the spindle neoplastic cells concentrically surrounded non-dilated native renal tubules, of creating an onion-skin pattern similar to that described in renal metanephric stromal tumor¹⁸ (Figure 1H). In case 2, only focal microscopic dilation of entrapped renal tubules was evident at the periphery of the lesion (Figure 2H). Instead, this lesion was predominantly solid and had more aggressive growth pattern featuring hemorrhage, necrosis, and renal sinus vascular invasion along with perinephric fat invasion approaching the adrenal gland (Figure 2I, 2J).

The immunohistochemical profiles were not specific. By immunohistochemistry, both neoplasms labeled for CD56 and BCL2. CD99 showed diffuse but nonspecific cytoplasmic staining. Both neoplasms demonstrated focal labeling for WT-1 (nuclear), TLE1, synaptophysin, estrogen receptor, and cyclin D1. Of note, the extent of labeling for TLE1 and cyclin D1 was greater in case 1 (50–60%) than in case 2 (5–10%).

Both neoplasms were negative for PAX8, myogenin, actin, inhibin, S100, CD34, HMB45, cytokeratin, and GFAP. Desmin labeled only rare cells in case 1 and was completely negative in case 2. Of note, the entrapped renal tubules and cysts of case 1 labeled as expected for PAX8. BCOR was immunoreactive in case one in approximately 60% of neoplastic cells with moderate intensity, but was negative in case 2. SATB2 labeled rare cells in case one but not case two.

RNA Sequencing

In case 1 (the index case), RNA sequencing identified 2 different fusion transcript variants, equally expressed, in which *MEIS1* exon 7 fused to either *NCOA2* exon 13 or 14 (Fig. 3A,B).

FISH

FISH analysis confirmed *MEIS1-NCOA2* renal sarcoma case 2, showing break-apart signal in both *NCOA2* and *MEIS1* genes (Fig. 4). FISH analysis also validated the RNA sequencing candidate fusions in *MEIS1-NCOA2* renal sarcoma case 1 (not shown).

MEIS1-NCOA2 positive kidney sarcoma grouped closely to HEY1-NCOA2 positive mesenchymal chondrosarcomas by unsupervised clustering of RNA sequencing.

By unsupervised hierarchical clustering, the renal *MEIS1-NCOA2* sarcoma case 1 grouped together with the 2 mesenchymal chondrosarcomas harboring *HEY1-NCOA2* available on the same targeted RNA sequencing platform, and away from one soft tissue angiofibroma with *AHRR-NCOA2* fusion (Fig. 3C). The *MEIS1* gene was not one of the targeted genes included in the RNA sequencing panel and thus we were not able to evaluate the *MEIS1* mRNA expression in our cohort. However, both *HEY1* and *AHRR* genes were included in the panel, and showed a high level of expression in both mesenchymal chondrosarcoma and soft tissue angiofibroma, respectively, but not in the renal *MEIS1-NCOA2* sarcoma case 1 (Fig. 3D). Furthermore, we investigated the differential expression of *NCOA2* gene, which showed high expression of 3' *NCOA2* exons participating in the fusion (exons 13–23) in tumors showing *NCOA2* gene fusion regardless of its partners (Fig. 3E).

Given the known fusion of *HEY1* and *NCOA2* in mesenchymal chondrosarcoma¹⁹, we sought to determine if some mesenchymal chondrosarcomas have *MEIS1* rather than *HEY1* as the *NCOA2* partner. However, none of the 4 mesenchymal chondrosarcomas with known *NCOA2* gene rearrangement demonstrated *MEIS1* gene rearrangements.

Mixed epithelial stromal tumor of the kidney/Cystic Nephroma do not harbor MEIS1-NCOA2 gene fusions

Given the extensively cystic appearance of *MEIS1-NCOA2* renal sarcoma case 1, along with the complex patterns of entrapped native renal tubules within the lesion, one diagnostic consideration was that of a sarcoma arising within a mixed epithelial stromal tumor/cystic nephroma (MEST/CN). Therefore, we examined a group of 11 typical MEST/CN along with 2 pediatric CN for *MEIS1-NCOA2* gene fusions by FISH. However, none of these neoplasms demonstrated evidence of *NCOA2* or *MEIS1* gene rearrangements.

DISCUSSION

We describe what we believe to be a novel subtype of sarcoma involving the kidney in two adult patients. The neoplasm characteristically demonstrates nodular variations in cellularity with distinctive whorling of the monomorphic spindle cells with pale eosinophilic cytoplasm. In addition a variable component of primitive small round cells was also noted showing a perivascular distribution. Most significantly, these two morphologically similar neoplasms demonstrate an identical, previously undescribed *MEIS1-NCOA2* gene fusion.

The *NCOA2* (nuclear receptor co-activator 2) gene is located on chromosome 8q13, and encodes for a nuclear hormone receptor transcriptional co-activator^{20,21}. *NCOA2* interacts with ligand-bound receptors to recruit histone acetyltransferases and methyltransferases to facilitate chromatin remodeling and transcription. *NCOA2* has previously been implicated as a 3' partner in gene fusions in sarcomas and leukemias (see below), in which the C-terminal transcriptional activation domains 1 and 2 have been consistently retained in the predicted fusion proteins. Hence, the postulated consequence of these translocations is that *NCOA2* is aberrantly targeted by a novel DNA-binding domain contributed by its N-terminal partner¹⁹.

While occasional cases of acute myeloid leukemia have been associated with either *MYST3-NCOA2*²² or *ETV6-NCOA2*²³ gene fusion, a larger number of mesenchymal neoplasms have been shown to be associated with *NCOA2* gene fusions. The main differential diagnostic consideration for our *MEIS1-NCOA2* renal sarcomas is that of an unusual mesenchymal chondrosarcoma which harbors an alternative *MEIS1-NCOA2* gene fusion rather than the canonical *HEY1-NCOA2* gene fusion that most mesenchymal chondrosarcomas harbor. Several lines of evidence argue against this alternative possibility. First, the cytology of the *MEIS1-NCOA2* renal sarcomas is that of a monotonous spindle neoplasm rather than primitive small blue round cells seen in mesenchymal chondrosarcoma (Fig. 5). Second, mesenchymal chondrosarcoma is consistently negative for TLE1 by immunohistochemistry,^{24,25} while both of our *MEIS1-NCOA2* renal sarcomas were positive. Third, we found no evidence of *MEIS1* rearrangement in a group of mesenchymal chondrosarcomas with confirmed *NCOA2* gene rearrangement.

NCOA2 gene fusions are also characteristic of congenital/infantile spindle cell rhabdomyosarcoma, with various partners, including *VGLL2*, *SRF*, or *TEAD1*, which represent critical transcription factors or co-activators involved in muscle development and regulation^{26, 27}. Of note, *NCOA2*-fusion positive infantile spindle cell rhabdomyosarcomas have a favorable prognosis compared to the older childhood and adult sclerosing/spindle cell rhabdomyosarcomas associated with *MYOD1* mutations²⁸. Rare cases of alveolar rhabdomyosarcoma have been associated with *PAX3-NCOA2* gene fusions²⁹. While one of our *MEIS1-NCOA2* renal sarcomas demonstrated rare desmin-positive cells, the rhabdomyosarcomas referred to above consistently label for muscle markers such as myogenin and actin and label more diffusely for desmin.

Another soft tissue tumor recently shown to harbor recurrent *NCOA2* gene rearrangements is the so-called soft tissue angiofibroma, characterized by an *AHRR-NCOA2* gene fusion, with occasional cases demonstrating a *GTF21-NCOA2* gene fusion³⁰⁻³⁴. Soft tissue

angiofibroma typically occurs in adult females, and features bland spindle cells associated with prominent thin-walled hemangiopericytomatous vessels with fibrinoid change and thick collagen. Soft tissue angiofibroma lacks the overt sarcomatous appearance of *MEIS1-NCOA2*-positive renal tumors, while the latter lacks the characteristic vasculature of soft tissue angiofibroma.

In the current neoplasms, the *NCOA2* partner is *MEIS1*, which encodes for a 390 amino acid protein, located at chromosome 2p14. *MEIS1* is a member of the three amino acid loop extension (TALE) homeodomain transcription factor family, and is thought to activate target genes by association with Hox transcription factors. *MEIS1* stands for ‘*myeloid ectopic viral integration site-1*’ and its overexpression, induced by retroviral integration, leads to myeloid leukemia. *MEIS1* is thought to have roles in cardiac regeneration, stem cell function and tumorigenesis^{35,36}. In some neoplasms such as clear cell renal cell carcinoma, prostatic adenocarcinoma and esophageal squamous cell carcinoma^{37, 38}, *MEIS1* functions as a tumor suppressor whereas in others it functions as an oncogene. Along these lines, *MEIS1* is known to be amplified in a subset of malignant peripheral nerve sheath tumors³⁹ and neuroblastomas⁴⁰, overexpressed in ovarian cancers⁴¹, and act as co-factor with *HoxA9* in driving acute leukemias, particularly aggressive MLL-associated leukemias⁴² and chemotherapy-resistant leukemias^{43–45}. *MEIS1* has not previously been associated with chromosome translocations and resulting gene fusions in cancer.

While the partners of *NCOA2* in congenital/infantile spindle cell rhabdomyosarcoma (*SRF*, *VGLL-2*, and *TEAD1*) are genes that are normally expressed skeletal muscle, *MEIS1* is broadly expressed in a variety of human tissues, and therefore its tissue distribution would not account for preferential localization of this neoplasm in the kidney. Indeed, along these lines we found no evidence of expression of renal specific immunohistochemical markers (such as PAX8) in our renal neoplasms.

Within the kidney, the differential diagnosis of the *MEIS1-NCOA2* sarcomas is broad. The *BCOR-CCNB3* renal sarcomas¹² which overlap with CCSK have the greatest degree of morphologic overlap with the *MEIS1-NCOA2* sarcomas. Both neoplasms feature evenly-placed, plump spindle cells with a regular capillary vascular pattern, and both label for immunohistochemical markers such as TLE1. One of our *MEIS1-NCOA2* renal sarcomas was positive for BCOR⁴⁶: while this neoplasm demonstrated moderate-strong reactivity in approximately 60% of nuclei, it was less than the diffuse strong labeling typically seen in sarcomas harboring *BCOR* genetic alterations, such as *BCOR* internal tandem duplication or the *BCOR-CCNB3* gene fusion^{47,48}. Aside from genetics, the key morphologic feature of the *MEIS1-NCOA2* neoplasms is the nodular variation in cellularity associated with spindle cell whorling and clustering of the small cells. Some areas of the *MEIS1-NCOA2* renal sarcomas are morphologically identical to the appearance of monophasic synovial sarcoma, and both may label for BCOR and TLE1. Aside from the distinctive *SS18-SSX* gene fusions, renal synovial sarcoma typically demonstrates more elongated, hyperchromatic nuclei, and lacks the nodular variations in cellularity seen in the *MEIS1-NCOA2* renal sarcomas. The nodularity and focal onionskin pattern noted raised the differential diagnosis of metanephric stromal tumor (MST)¹⁸. However, MST typically labels for CD34, and demonstrates characteristic features (such as angiodysplasia, glial-epithelial complexes) not

seen in the two *MEIS1-NCOA2* renal sarcomas. The recently described *CIC*-rearranged renal sarcomas⁴⁹ also enter into the differential diagnosis, and these may also be immunoreactive for WT1 in approximately 50% of cases. The *CIC*-associated sarcomas typically have more variable round to epithelioid cell cytology, prominent nucleoli and myxoid matrix. The primitive solid areas of case # 2 raise the differential diagnosis of a Ewing sarcoma/primitive neuroectodermal family tumor, but the spindling as well as absence of diffuse membranous CD99 immunoreactivity excluded that possibility. The predominantly cystic appearance of case 1 raised the differential diagnosis of biphasic cystic renal neoplasms including mixed epithelial stromal tumor/Cystic Nephroma (MEST/CN)⁵⁰ and angiomyolipoma with epithelial cysts (AMLEC)⁵¹. However, the former are associated with more diffuse immunoreactivity for estrogen receptor than is seen in the current cases, demonstrate “ovarian-like,” cellular stroma with wavy collagen which is immunoreactive for inhibin in most cases, and are typically immunoreactive for muscle markers. None of the MEST/CN cases tested demonstrated *NCOA2* gene rearrangements. Unlike the *MEIS1-NCOA2* sarcomas, AMLEC labels for melanocytic markers such as HMB45 and Melan A.

In summary, we describe a distinctive sarcoma subtype in the kidney harboring novel *MEIS1-NCOA2* gene fusions, characterized by plump spindle cells with variable amounts of eosinophilic cytoplasm demonstrating prominent nodular variations in cellularity. Further studies will be needed to determine the full clinicopathologic and morphologic spectrum of this distinctive neoplasm. We have minimal clinical follow-up in these cases. However, the primitive cytology and mitotic activity of both cases, along with the cellular necrosis, vascular invasion and perinephric fat invasion demonstrated by case 2, strongly suggests that they have malignant potential.

Supplementary Material

Refer to Web version on PubMed Central for supplementary material.

Acknowledgement:

We thank Norman Barker MA, MS, RBP for expert photographic assistance.

Disclosures: Supported in part by: P50 CA 140146–01 (CRA), P30-CA008748 (CRA), Cycle for Survival (CRA), Kristin Ann Carr Foundation (CRA), Dahan Translocation Carcinoma Fund (PA), Joey’s Wings (PA)

REFERENCES

1. Knezevich SR, Garnett MJ, Pysher TJ, et al. *ETV6-NTRK3* gene fusions and trisomy 11 establish a histogenetic link between mesoblastic nephroma and congenital fibrosarcoma. *Cancer Res* 1998; 58:5046–5048. [PubMed: 9823307]
2. Rubin BP, Chen CJ, Morgan TW, et al. Congenital mesoblastic nephroma t(12;15) is associated with *ETV6-NTRK3* gene fusion: cytogenetic and molecular relationship to congenital (infantile) fibrosarcoma. *Am J Pathol* 1998; 153:1451–1458. [PubMed: 9811336]
3. Argani P, Fritsch M, Kadkol SS, et al. Detection of the *ETV6-NTRK3* chimeric RNA of infantile fibrosarcoma/cellular congenital mesoblastic nephroma in paraffin-embedded tissue: application to challenging pediatric renal stromal tumors. *Mod Pathol* 2000; 13:29–36. [PubMed: 10658907]
4. Quezado M, Benjamin DR, Tsokos M EWS/FLI-1 fusion transcripts in three peripheral primitive neuroectodermal tumors of the kidney. *Hum Pathol* 1997; 28:767–771. [PubMed: 9224742]

5. Jimenez RE, Folpe AL, Lapham RL, et al. Primary Ewing's sarcoma/primitive neuroectodermal tumor of the kidney. A clinicopathologic and immunohistochemical analysis of 11 cases. *Am J Surg Pathol* 2002; 26:320–327. [PubMed: 11859203]
6. Argani P, Faria PA, Epstein JI, et al. Primary renal synovial sarcoma. Morphologic and molecular delineation of an entity previously included among embryonal sarcomas of the kidney. *Am J Surg Pathol* 2000; 24:1087–1096. [PubMed: 10935649]
7. Argani P, Lewin JR, Edmonds P, Netto GJ, Prieto Granada, Zhang L, Jungbluth AA, Antonescu CR Primary renal sclerosing epithelioid fibrosarcoma: report of 2 cases with EWSR1-CREB3L1 gene fusion. *Am J Surg Pathol*. 2015; 39:365–73. [PubMed: 25353281]
8. Wang LL, Perlman EJ, Vujanic GM, et al. Desmoplastic small round cell tumor of the kidney in childhood. *Am J Surg Pathol* 2007; 31:576–584. [PubMed: 17414105]
9. Rubin BP, Fletcher JA, Renshaw AA Clear cell sarcoma of soft parts: report of a case primary in the kidney with cytogenetic confirmation. *Am J Surg Pathol* 1999; 23:589–94. [PubMed: 10328092]
10. Argani P, Aulmann S, Illei PB, Netto GJ, Ro J, Cho HY, Dogan S, Ladanyi M, Martignoni G, Goldblum JR, Weiss SW A distinctive subset of PEComas harbors TFE3 gene fusions. *Am J Surg Pathol*. 2010; 34:1395–406. [PubMed: 20871214]
11. Argani P, Aulmann S, Karanjawala Z, Fraser RB, Ladanyi M, Rodriguez MM Melanotic Xp11 translocation renal cancers: a distinctive neoplasm with overlapping features of PEComa, carcinoma, and melanoma. *Am J Surg Pathol*. 2009; 33:609–19. [PubMed: 19065101]
12. Argani P, Kao Y-C, Zhang L, Bacchi C, Matoso A, Alaggio R, Epstein JI, Antonescu CR Primary Renal Sarcomas with BCOR-CCNB3 Gene Fusion: A Report of Two Cases Showing Histologic Overlap with Clear Cell Sarcoma of Kidney, Suggesting Further Link Between BCOR-related Sarcomas of the Kidney and Soft Tissues. *Am J Surg Pathol* 2017; 41:1702–1712. [PubMed: 28817404]
13. O'Meara E, Stack D, Lee CH, Garvin J, Morris T, Argani P, Han J, Gisselson D, Leuschner I, Gessler M, Graf N, Fletcher JA, O'Sullivan MJ Characterization of the chromosome translocation t(10;17)(q22;p13) in clear cell sarcoma of kidney. *J Pathol* 2012; 227: 72–80. [PubMed: 22294382]
14. Ueno-Yokohata H, Okita H, Nakasato K, et al. Consistent in-frame internal tandem duplications of BCOR characterize clear cell sarcoma of the kidney. *Nat Genet*. 2015; 47:861–863. [PubMed: 26098867]
15. Antonescu CR, Zhang L, Chang NE, et al. EWSR1-POU5F1 fusion in soft tissue myoepithelial tumors. A molecular analysis of sixty-six cases, including soft tissue, bone, and visceral lesions, showing common involvement of the EWSR1 gene. *Genes Chromosomes Cancer*. 2010; 49:1114–1124. [PubMed: 20815032]
16. Antonescu CR, Agaram NP, Sung YS, Zhang L, Swanson D, Dickerson BC A Distinct Malignant Epithelioid Neoplasm with GLI1 Gene Rearrangements, Frequent S100 Protein Expression, and Metastatic Potential: Expanding the Spectrum of Pathologic Entities with ACTB/MALAT1/PTCH1-GLI1 Fusions. *Am J Surg Pathol* 2018; 42:553–560. [PubMed: 29309307]
17. Li Y, Pawel BR, Hill DA, Epstein JI, Argani P Pediatric cystic nephroma is morphologically, immunohistochemically, and genetically distinct from adult cystic nephroma. *Am J Surg Pathol* 2017; 41:472–481. [PubMed: 28177962]
18. Argani P, Beckwith JB Metanephric stromal tumor: report of 31 cases of a distinctive pediatric renal neoplasm. *Am J Surg Pathol* 2000; 24:917–26. [PubMed: 10895814]
19. Wang L, Motoi T, Khanin R, Olshen A, Mertens F, Bridge J, Dal Cin P, Antonescu CR, Singer S, Hameed M, Bovee JV, Hogendoorn PC, Socci N, Ladanyi M Identification of a novel, recurrent HEY1-NCOA2 fusion in mesenchymal chondrosarcoma based on a genome-wide screen of exon-level expression data. *Genes Chromosomes Cancer*. 2012; 51:127–39. [PubMed: 22034177]
20. Koh SS, Chen D, Lee YH, Stallcup MR Synergistic enhancement of nuclear receptor function by p160 coactivators and two coactivators with protein methyltransferase activities. *J Biol Chem* 2001; 276:1089–98.
21. Chen D, Ma H, Hong H, Koh SS, Huang SM, Schurter BT, Asward DW, Stallcup MR Regulation of transcription by a protein methyltransferase. *Science* 1999; 285:2175–7.

22. Troke PF, Kindle KB, Collins HM, Heery DM MOZ fusion proteins in acute myeloid leukemia. *Biochem Soc. Symp* 2006 73:23–39.
23. Strehl S, Nebral K, König M, Harbott J, Strobl H, Ratei R, Struski S, Bielora B, Lessard M, Zimmermann M, Haas OA, Izraeli S ETV6-NCOA2: a novel fusion gene in acute leukemia associated with coexpression of T-lymphoid and myeloid markers and frequent NOTCH1 mutations. *Clin Cancer Res* 2008; 15:977–83.
24. Terry J, Saito T, Subramanian S, Ruttan C, Antonescu CR, Goldblum JR, Downs-Kelly E, Corless CL, Rubin BP, van de Rijn M, Ladanyi M, Nielsen TO TLE1 as a diagnostic immunohistochemical marker for synovial sarcoma emerging from gene expression profiling studies. *Am J Surg Pathol* 2007; 31:240–6. [PubMed: 17255769]
25. He X, Xiong B, Zhou T, Lan T, Chen M, Chen H, Peng R, Guo J, Zhang H Diagnostic value of TLE1 for synovial sarcoma: immunohistochemical analyses of genetically confirmed synovial sarcomas and nonsynovial sarcomas. *Int J Clin Exp Pathol* 2016; 9:4339–4350.
26. Mosquera JM, Sboner A, Zhang L, Kitabayashi N, Chen CL, Sung YS, Wexler LH, LaQuaglia MP, Edelman M, Sreekantaiah C, Rubin MA, Antonescu CR Recurrent NCOA2 gene rearrangements in congenital/infantile spindle cell rhabdomyosarcoma. *Genes Chromosomes Cancer*. 2013; 52:538–50. [PubMed: 23463663]
27. Alaggio R, Zhang L, Sung YS, Huang SC, Chen CL, Bisogno G, Zin A, Agaram NP, LaQuaglia MP, Wexler LH, Antonescu CR A Molecular Study of Pediatric Spindle and Sclerosing Rhabdomyosarcoma: Identification of Novel and Recurrent VGLL2-related Fusions in Infantile Cases. *Am J Surg Pathol*. 2016; 40:224–35 [PubMed: 26501226]
28. Agaram NP, Chen CL, Zhang L, LaQuaglia MP, Wexler L, Antonescu CR Recurrent MYOD1 mutations in pediatric and adult sclerosing and spindle cell rhabdomyosarcomas: evidence for a common pathogenesis. *Genes Chromosomes Cancer*. 2014; 53:779–87 [PubMed: 24824843]
29. Sumegi J, Streblov R, Frayer RW, Dal Cin P, Rosenberg A, Meloni-Ehrig A, Bridge JA Recurrent t(2;2) and t(2;8) translocations in rhabdomyosarcoma without the canonical PAX-FOXO1 fuse PAX3 to members of the nuclear receptor transcriptional coactivator family. *Genes Chromosomes Cancer*. 2010; 49:224–36. [PubMed: 19953635]
30. Panagopoulos I, Gorunova L, Viset T, Heim S Gene fusions AHRR-NCOA2, NCOA2-ETV4, ETV4-AHRR, P4HA2-TBCK, and TBCK-P4HA2 resulting from the translocations t(5;8;17)(p15;q13;q21) and t(4;5)(q24;q31) in a soft tissue angiofibroma. *Oncol Rep*. 2016; 36:2455–2462. [PubMed: 27633981]
31. Jin Y, Möller E, Nord KH, Mandahl N, Von Steyern FV, Domanski HA, Mariño-Enríquez A, Magnusson L, Nilsson J, Sciot R, Fletcher CD, Debiec-Rychter M, Mertens F Fusion of the AHRR and NCOA2 genes through a recurrent translocation t(5;8)(p15;q13) in soft tissue angiofibroma results in upregulation of aryl hydrocarbon receptor target genes. *Genes Chromosomes Cancer*. 2012; 51:510–20. [PubMed: 22337624]
32. Bekers EM, Groenen PJ, Verdijk MA, Raaijmakers-van Geloof WL, Roepman P, Vink R, Gilhuijs ND, van Gorp JM, Bovée JV, Creyten DH, Flanagan AM, Suurmeijer AJ, Mentzel T, Arbajian E, Flucke U Soft tissue angiofibroma: Clinicopathologic, immunohistochemical and molecular analysis of 14 cases. *Genes Chromosomes Cancer*. 2017; 56:750–757. [PubMed: 28639284]
33. Yamada Y, Yamamoto H, Kohashi K, Ishii T, Iura K, Maekawa A, Bekki H, Otsuka H, Yamashita K, Tanaka H, Hiraki T, Mukai M, Shirakawa A, Shinnou Y, Jinno M, Yanai H, Taguchi K, Maehara Y, Iwamoto Y, Oda Y Histological spectrum of angiofibroma of soft tissue: histological and genetic analysis of 13 cases. *Histopathology*. 2016;69:459–6 [PubMed: 26845637]
34. Sugita S, Aoyama T, Kondo K, Keira Y, Ogino J, Nakanishi K, Kaya M, Emori M, Tsukahara T, Nakajima H, Takagi M, Hasegawa T Diagnostic utility of NCOA2 fluorescence in situ hybridization and Stat6 immunohistochemistry staining for soft tissue angiofibroma and morphologically similar fibrovascular tumors. *Hum Pathol*. 2014; 45:1588–96. [PubMed: 24856853]
35. Aksoz M, Turan RD, Albayrak E, Kocabas F Emerging Roles of Meis1 in Cardiac Regeneration, Stem Cells and Cancer. *Curr Drug Targets*. 2018; 19:181–190. [PubMed: 28745213]
36. Blasi F, Bruckmann C, Penkov D, Dardaei L A tale of TALE, PREP1, PBX1, and MEIS1: Interconnections and competition in cancer. *Bioessays*. 2017; 39.

37. Zhu J, Cui L, Xu A, Yin x, Li F, Gao J. MEIS1 inhibits clear cell renal cell carcinoma cells proliferation and in vitro invasion or migration. *BMC Cancer* 2017; 17:176. [PubMed: 28270206]
38. Rad A, Farshcian M, Forghanifard MM, Matin MM, Bahrami AR, Geerts D, A'rabi A, Memar B, Abbaszadegan MR Predicting the molecular role of MEIS1 in esophageal squamous cell carcinoma. *Tumour Biol* 2016; 37:1715–25. [PubMed: 26314854]
39. Patel AV, Chaney KE, Choi K, Largaespada DA, Kumar AR, Ratner N An ShRNA screen identifies MEIS1 as a driver of malignant peripheral nerve sheath tumors. *EBioMedicine* 2016; 9:110–119. [PubMed: 27333032]
40. Jones TA, Flomen RH, Senger G, Nizeti D, Sheer D The homeobox gene MEIS1 is amplified in IMR-32 and highly expressed in other neuroblastoma cell lines. *Eur J Cancer* 2000; 36:2368–74. [PubMed: 11094311]
41. Crijns AP, de Graeff P, Geerts D, Ten Hoor KA, Hollema H, van der Sluis T, Hofstra RM, de Bock GH, de Jong S, van der Zee AG, de Vries EG MEIS and PBX homeobox proteins in ovarian cancer. *Eur J Cancer* 2007 43:2495–505. [PubMed: 17949970]
42. Liu J, Qin YZ, Yang S Wang, Chang YJ, Zhao, Jiang, Huang Meis1 is critical to the maintenance of human acute myeloid leukemia cells independent of MLL rearrangements. *Ann Hematol* 2017 96:567–574. [PubMed: 28054140]
43. Rosales-Avina JA, Torres-Flores J, Aguilar-Lemarroy A, Gurrola-Díaz C Hernández-Flores G, Oritiz-Larareno PC, Lerma-Díaz JM, de Celis R, González-Ramella O, Barrera-Chaires E, Bravo-Cuellar A, Jave-Suárez LF MEIS1, PREP1, and PBX4 are differentially expressed in acute lymphoblastic leukemia: association of MEIS1 expression with higher proliferation and chemotherapy resistance. *J Exp Clin Cancer Res* 2011; 20:30:112.
44. Wong P, Iwasaki M, Somerville TC, So CW, Cleary ML Meis1 is an essential and rate-limiting regulator of MLL leukemia stem cell potential. *Genes Dev.* 2007; 21:2762–74. [PubMed: 17942707]
45. Collins CT, Hess JL Deregulation of the HOXA9/MEIS1 axis in acute leukemia. *Curr Opin Hematol.* 2016; 23:354–61 [PubMed: 27258906]
46. Kao YC, Sung YS, Zhang L, Jungbluth AA, Huang SC, Argani P, Agaram NP, Zin A, Alaggio R, Antonescu CR BCOR Overexpression Is a Highly Sensitive Marker in Round Cell Sarcomas With BCOR Genetic Abnormalities. *Am J Surg Pathol* 2016; 40:1670–1678. [PubMed: 27428733]
47. Argani P, Pawel B, Szabo S, Reyes-Múgica M, Timmons C, Antonescu CR Diffuse Strong BCOR Immunoreactivity is a Sensitive and Specific Marker for Clear Cell Sarcoma of the Kidney (CCSK) in Pediatric Renal Neoplasia. *Am J Surg Pathol* 2018;42: 1128–31. [PubMed: 29851702]
48. Kao YC, Sung YS, Zhang L, Huang SC, Argani P, Chung CT et al. Recurrent BCOR Internal Tandem Duplication and YWHAE-NUTM2B Fusions in Soft Tissue Undifferentiated Round Cell Sarcoma of Infancy: Overlapping Genetic Features With Clear Cell Sarcoma of Kidney. *Am J Surg Pathol* 2016; 40:1009–20. [PubMed: 26945340]
49. Mangray S, Kelly D, LeGuellec S, Fridman E, Mary Shago M, Matoso A, Madison R, Zhong S, Li R, Lombardo KA, Pressey J, Cramer S, Ross JS, Corona RJ, Bratslavsky G, Argani P, Coindre J-M, Ali, Yakirevich E. Clinicopathologic Features of a Series of Primary Renal CIC-rearranged Sarcomas with Comprehensive Molecular Analysis. *Am J Surg Pathol* 2018 6 12 [Epub ahead of print]
50. Caliò A, Eble JN, Grignon DJ, Delahunt B Mixed Epithelial and Stromal Tumor of the Kidney: A Clinicopathologic Study of 53 Cases. *Am J Surg Pathol.* 2016;40:1538–1549 [PubMed: 27635943]
51. Fine SW, Reuter VE, Epstein JI, Argani P Angiomyolipoma with epithelial cysts (AMLEC): a distinct cystic variant of angiomyolipoma. *Am J Surg Pathol.* 2006; 30:593–9. [PubMed: 16699313]

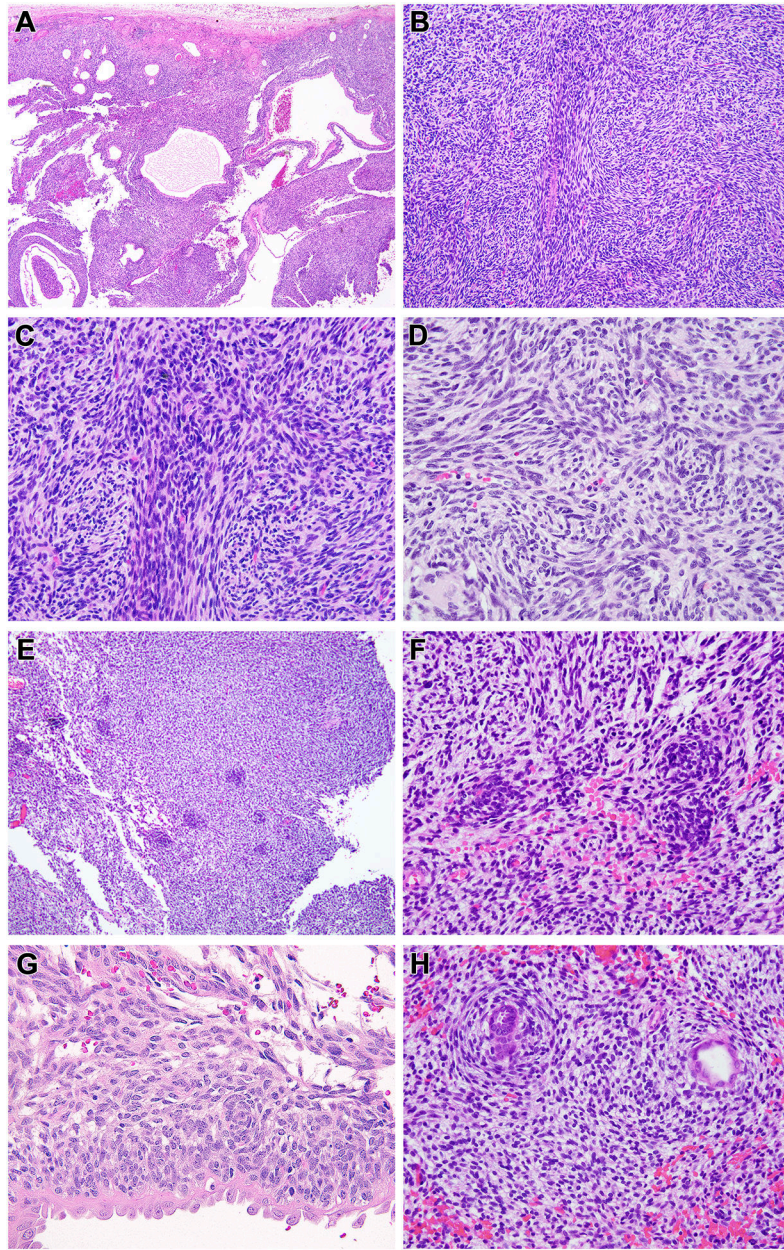


Figure 1. Morphologic features of renal case 1 with *MEIS1-NCOA2* fusion (index case). This neoplasm had a dominant cystic appearance at low power (A), created by a solid spindle cell neoplasm associated with entrapped cystically-dilated renal tubules. The neoplasm had a nodular low power appearance (B) created by centrally located spindle cells with more abundant eosinophilic cytoplasm separated by primitive spindle to epithelioid cells with scant cytoplasm (C). The cytology in these areas overlapped with that of monophasic synovial sarcoma. The centrally located spindle cells demonstrated whorling (D). Small primitive cells arranged in clusters (E) and vague whorling similar to the spindle cells (F). The primitive neoplastic cells were cytologically distinct from the entrapped, cystically-dilated native renal tubular epithelium, which had more open, vesicular chromatin

and hobnail appearance (G). In focal areas the spindle cells encircled native tubules in a concentric, “onion-skin” pattern (H).

Author Manuscript

Author Manuscript

Author Manuscript

Author Manuscript

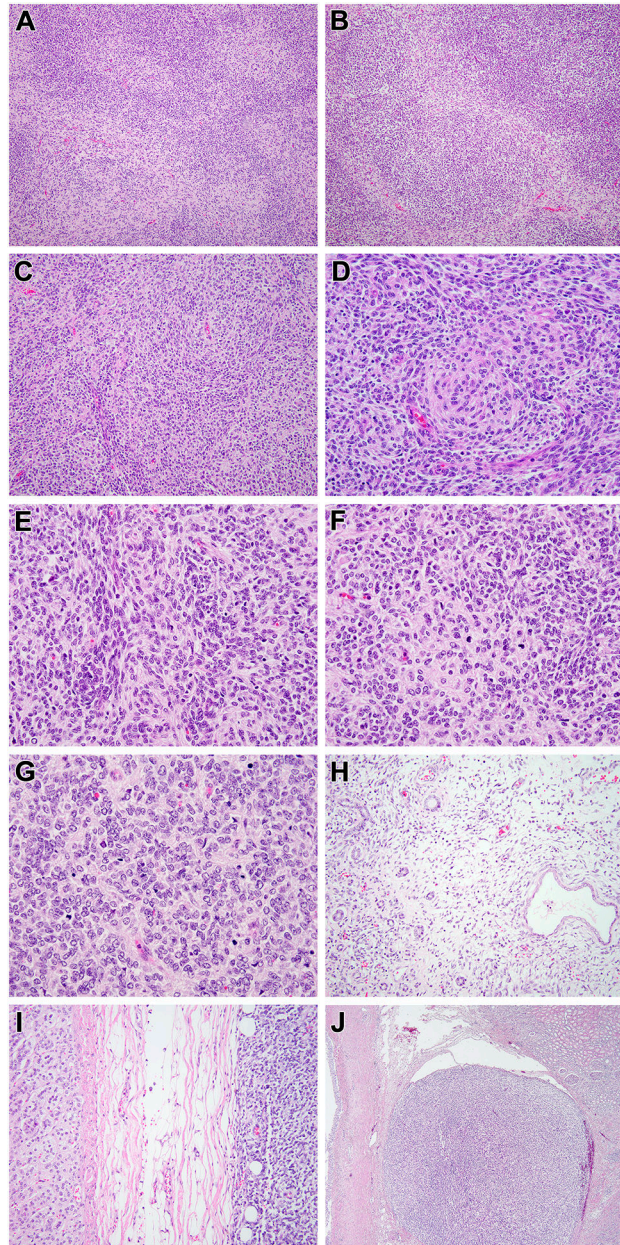


Figure 2. Morphologic features of renal case 2 with *MEIS1-NCOA2* fusion.

This solid cellular neoplasm had distinctive nodular variations in cellularity as evident at low power (A). In some areas, the nodularity was created by hypocellular fibrous zones separating more cellular nodules (B). The most consistent pattern, as seen in case 1, was that of centrally located spindle cells with eosinophilic cytoplasm forming whorls, surrounded by smaller cells with less cytoplasm (C, D); the smaller cells were packed in tight clusters, often centered on capillaries (E). Mitotic figures were readily identifiable in both components (F). In more cellular areas, the appearance resembles that of a small blue round cell tumor such as a primitive neuroectodermal tumor (PNET) with Homer Wright rosettes (G). This solid cellular neoplasm focally permeated between native renal tubules at its periphery but a significant cystic component was absent (H). The neoplasm invaded through

the renal capsule to approach the adrenal gland (I) and showing invasion into the renal sinus (J).

Author Manuscript

Author Manuscript

Author Manuscript

Author Manuscript

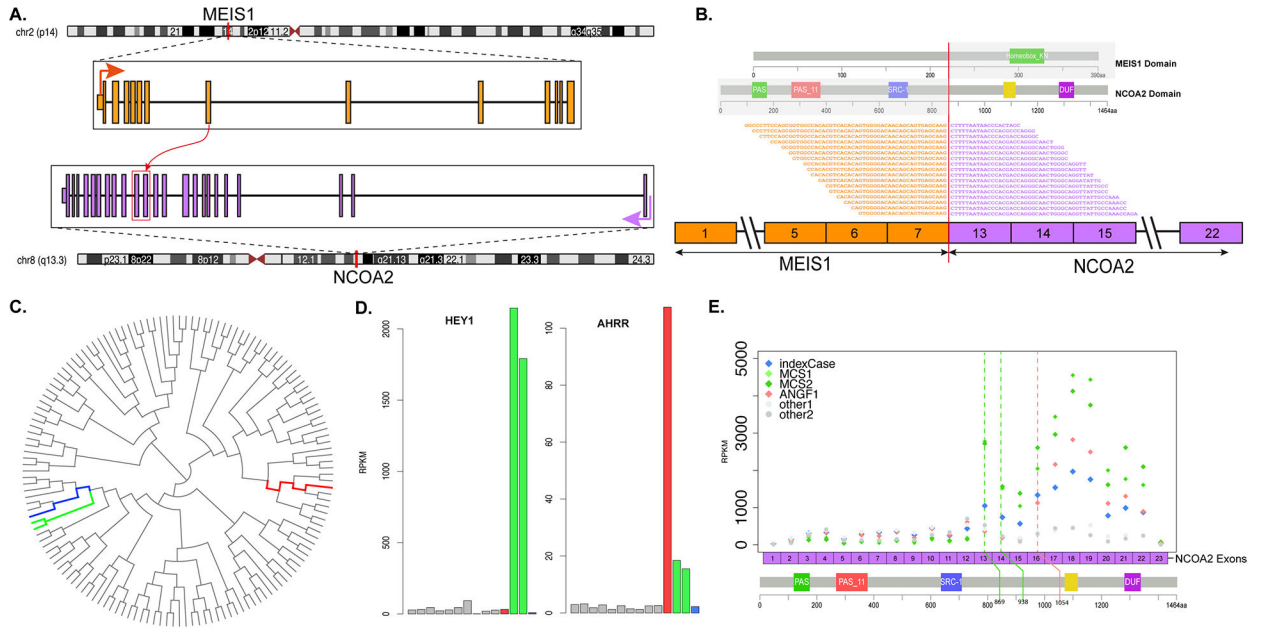


Figure 3. *MEIS1-NCOA2* gene fusion structure and molecular correlates. Diagrammatic representation of *MEIS1* gene on 2p14 fused to *NCOA2* gene on 8q13.3 (A). RNAseq reads identified 2 fusion transcript isoforms, in which exon 7 of *MEIS1* was fused (curved red arrow) to either exon 13 or 14 of *NCOA2* (red box), likely due to alternative splicing. Representative sequences from RNAseq data demonstrating the fusion of exon 7 of *MEIS1* to exon 13 of *NCOA2*, with emphasis on which protein domains are projected to be retained in the fusion oncoprotein (B). Unsupervised hierarchical clustering of RNAseq data showing that the *MEIS1-NCOA2* renal sarcoma case 1 (blue) clustered together with the 2 mesenchymal chondrosarcomas with *HEY1-NCOA2* fusion (green), separate from a soft tissue angiofibroma with *AHRR-NCOA2* fusion (red)(C); gray lines refer to a large cohort of various sarcoma types studied on the same targeted RNAseq platform (C). Bar chart of *HEY1* and *AHRR* mRNA expression showing upregulation in the mesenchymal chondrosarcomas and soft tissue angiofibroma, respectively, but not in *MEIS1-NCOA2* positive renal sarcoma case 1 (D). Exon level expression of *NCOA2* mRNA showing upregulation of the 3’end of *NCOA2* exons retained in the fusion transcript (breakpoints of renal sarcoma index case and 2 mesenchymal chondrosarcomas were identical in exons 13 and 14, green line; while breakpoint of angiofibroma in exon 16, red line)(E).

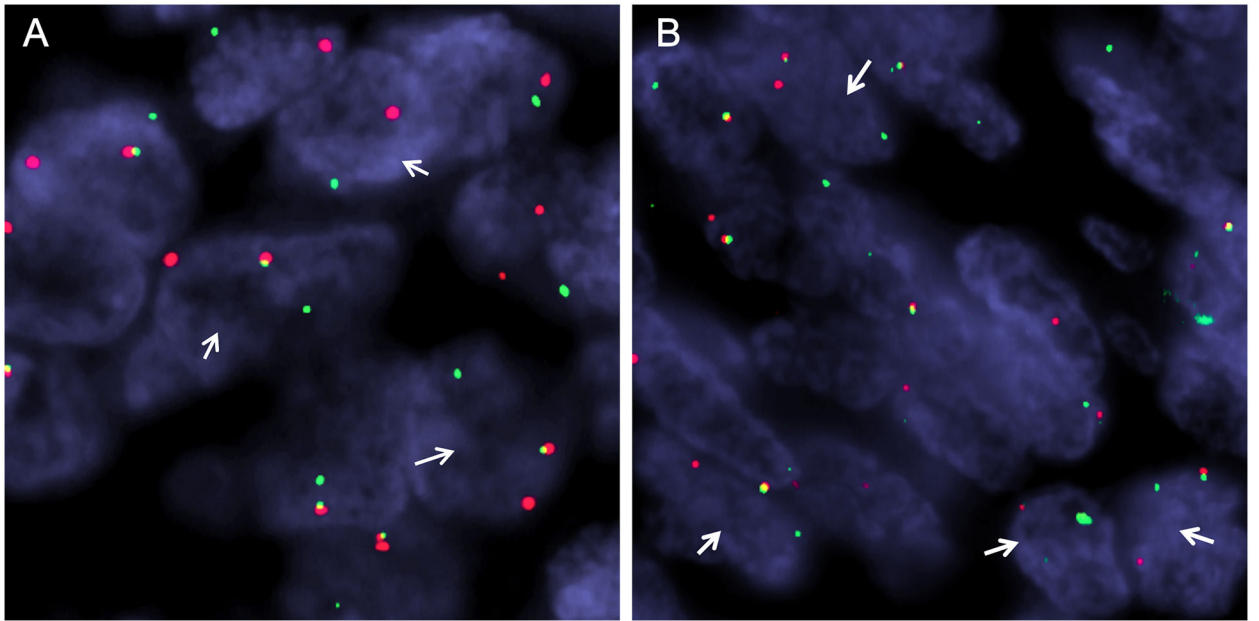


Figure 4. Break-apart FISH showing gene rearrangements in *MEIS1* and *NCOA2*. Renal sarcoma case 2 demonstrates rearrangement of *MEIS1* (A) and *NCOA2* (B) (red signal, centromeric; green signal, telomeric).

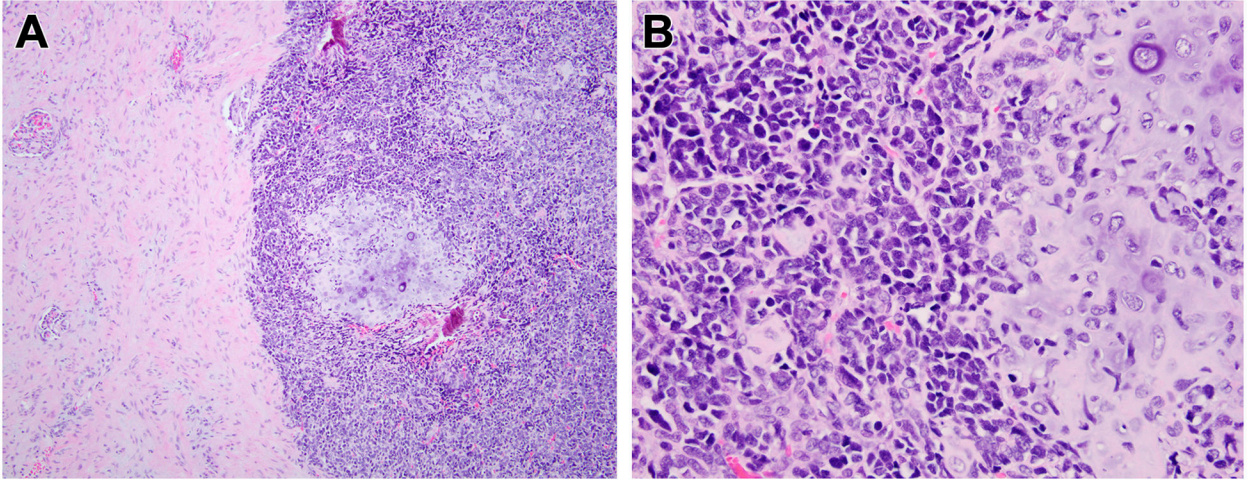


Figure 5. Histologic appearance of mesenchymal chondrosarcoma metastatic to the kidney for comparison.

At low power, one can appreciate the primitive small cells with associated nodules of cartilage to the right and entrapped kidney to the left (A). At high power (B), one can appreciate the cartilage and primitive small blue round cell appearance, which contrasts with the monomorphic spindle cell appearance of the *MEIS1-NCOA2* renal sarcomas. This mesenchymal chondrosarcoma showed a *NCOA2* gene rearrangement, but lacked evidence of *MEIS1* gene abnormalities.